Small-x behavior of deep-inelastic structure functions $\mathbf{F}_2$ and $\mathbf{F}_2^{cc}$

Anatoly Kotikov

Bogolubov Laboratory of Theoretical Physics, JINR, 141980 Dubna, Russia

It is shown that in the leading twist approximation of the Wilson operator product expansion with "frozen" and analytic strong coupling constants, Bessel-inspired behavior of the structure functions F_2 and F_2^{cc} at small x values, obtained for a flat initial condition in the DGLAP evolution equations, leads to good agreement with the deep inelastic scattering experimental data from HERA.

1 Introduction

The experimental data from HERA on the deep-inelastic scattering (DIS) structure function (SF) F_2 [1, 2], its derivative $\partial \ln F_2/\partial \ln(1/x)$ [3, 4] and the heavy quark parts F_2^{cc} and F_2^{bb} [5, 6, 7] enable us to enter into a very interesting kinematical range for testing the theoretical ideas on the behavior of quarks and gluons carrying a very low fraction of momentum of the proton, the so-called small-x region. In this limit one expects that the conventional treatment based on the Dokshitzer–Gribov–Lipatov–Altarelli–Parisi (DGLAP) equations [8] does not account for contributions to the cross section which are leading in $\alpha_s \ln(1/x)$ and, moreover, the parton distribution function (PDFs), in particular the gluon one, are becoming large and need to develop a high density formulation of QCD.

However, the reasonable agreement between HERA data and the next-to-leading-order (NLO) approximation of perturbative QCD has been observed for $Q^2 \geq 2$ GeV^2 (see reviews in [9] and references therein) and, thus, perturbative QCD could describe the evolution of F_2 and its derivatives up to very low Q^2 values, traditionally explained by soft processes.

The standard program to study the x behaviour of quarks and gluons is carried out comparing the experimental data with the numerical solution of the DGLAP equations [8] by fitting the QCD energy scale Λ and the parameters of the x-profile of partons at some initial Q_0^2 [10, 11]. However, to investigate exclusively the small-x region, there is the alternative of doing the simpler analysis by using some of the existing analytical solutions of DGLAP in the small-x limit [12]-[15]. It was pointed out in [12] that the HERA small-x data can be well interpreted in terms of the so-called doubled asymptotic scaling (DAS) phenomenon related to the asymptotic behaviour of the DGLAP evolution discovered many years ago [16].

The study of [12] was extended in [13]-[15] to include the finite parts of anomalous dimensions (ADs) of Wilson operators and Wilson coefficients[1]. This has led to predictions [14, 15] of the small-x asymptotic PDF form in the framework of the DGLAP dynamics, which were obtained starting at some Q_0^2 with the flat function

$$f_a(Q_0^2) \; = \; A_a \quad \text{(hereafter } a = q, g\text{)}, \tag{1}$$

[1] In the standard DAS approximation [16] only the AD singular parts were used.

where f_a are PDFs multiplied by x and A_a are unknown parameters to be determined from the data.

We refer to the approach of [13]-[15] as *generalized* DAS approximation. In this approach the flat initial conditions, Eq. (1), determine the basic role of the AD singular parts as in the standard DAS case, while the contribution from AD finite parts and from Wilson coefficients can be considered as corrections which are, however, important for better agreement with experimental data.

The use of the flat initial condition, given in Eq. (1), is supported by the actual experimental situation: low-Q^2 data [17, 18, 4] are well described for $Q^2 \leq 0.4$ GeV^2 by Regge theory with Pomeron intercept $\alpha_P(0) \equiv \lambda_P + 1 = 1.08$, closed to the adopted ($\alpha_P(0) = 1$) one. The small rise of HERA data [1, 2, 18, 19] at low Q^2 can be explained, for example, by contributions of higher twist operators (see [15]).

The purpose of this paper is to demostrate a good agreement [20, 21, 22] between the predictions of the generalized DAS approach [14] and the HERA experimental data [1, 2] (see Figs. 1 and 2 below) and [5, 7] (see Fig. 4 below) for the structure functions F_2 and F_2^{cc}, respectively. We also compare the result of the slope $\partial \ln F_2/\partial \ln(1/x)$ calculation with the H1 and ZEUS data [3, 4]. Looking at the H1 data [3] points shown in Fig. 3 one can conclude that $\lambda(Q^2)$ is independent on x within the experimental uncertainties for fixed Q^2 in the range $x < 0.01$. The rise of $\lambda(Q^2)$ linearly with $\ln Q^2$ could be tracted in strong nonperturbative way, i.e., $\lambda(Q^2) \sim 1/\alpha_s(Q^2)$. The analysis [23], however, demonstrated that this rise can be explained naturally in the framework of perturbative QCD.

The ZEUS and H1 Collaborations have also presented [4] the preliminary data for $\lambda(Q^2)$ at quite low values of Q^2. The ZEUS value for $\lambda(Q^2)$ is consistent with a constant ~ 0.1 at $Q^2 < 0.6$ GeV^2, as it is expected under the assumption of single soft Pomeron exchange within the framework of Regge phenomenology. It was important to extend the analysis of [23] to low Q^2 range with a help of well-known infrared modifications of the strong coupling constant. We used the "frozen" and analytic versions (see, [20]).

2 Generalized DAS approach

The flat initial condition (1) corresponds to the case when PDFs tend to some constant value at $x \to 0$ and at some initial value Q_0^2. The main ingredients of the results [14, 15], are:

- Both, the gluon and quark singlet densities [2] are presented in terms of two components (" + " and " − ") which are obtained from the analytic Q^2-dependent expressions of the corresponding (" + " and " − ") PDF moments.
- The twist-two part of the " − " component is constant at small x at any values of Q^2, whereas the one of the " + " component grows at $Q^2 \geq Q_0^2$ as

$$\sim e^{\sigma}, \quad \sigma = 2\sqrt{\left[\hat{d}_+ s - \left(\hat{D}_+ + \hat{d}_+ \frac{\beta_1}{\beta_0}\right) p\right] \ln\left(\frac{1}{x}\right)}\,, \quad \rho = \frac{\sigma}{2\ln(1/x)}\,, \tag{2}$$

  where σ and ρ are the generalized Ball–Forte variables,

$$s = \ln\left(\frac{a_s(Q_0^2)}{a_s(Q^2)}\right), \quad p = a_s(Q_0^2) - a_s(Q^2), \quad \hat{d}_+ = \frac{12}{\beta_0}, \quad \hat{D}_+ = \frac{412}{27\beta_0}. \tag{3}$$

[2] The contribution of valence quarks is negligible at low x.

Hereafter we use the notation $a_s = \alpha_s/(4\pi)$. The first two coefficients of the QCD β-function in the $\overline{\rm MS}$-scheme are $\beta_0 = 11 - (2/3)f$ and $\beta_1 = 102 - (114/9)f$ with f is being the number of active quark flavors.

Note here that the perturbative coupling constant $a_s(Q^2)$ is different at the leading-order (LO) and NLO approximations. Hereafter we consider for simplicity only the LO approximation[3], where the variables σ and ρ are given by Eq. (2) when $p = 0$.

2.1 Parton distributions and the structure function F_2

The SF F_2 and PDFs have the following form

$$F_2(x,Q^2) \;=\; e\, f_q(x,Q^2),\;\; f_a(x,Q^2) \;=\; f_a^+(x,Q^2) + f_a^-(x,Q^2),\;\; (a=q,g) \tag{4}$$

where $e = (\sum_1^f e_i^2)/f$ is the average charge square.

The small-x asymptotic results for PDFs $f_a^\pm$ are

$$\begin{aligned} f_g^+(x,Q^2) &= \left(A_g + \frac{4}{9}A_q\right) I_0(\sigma)\, e^{-\overline{d}_+(1)s} + O(\rho),\;\; f_q^+(x,Q^2) \;=\; \frac{f}{9}\frac{\rho I_1(\sigma)}{I_0(\sigma)} + O(\rho), \\ f_g^-(x,Q^2) &= -\frac{4}{9}A_q e^{-d_-(1)s} + O(x),\;\; f_q^-(x,Q^2) \;=\; A_q e^{-d_-(1)s} + O(x), \end{aligned} \tag{5}$$

where I_ν ($\nu = 0, 1$) are the modified Bessel functions, $d_-(1) = 16f/(27\beta_0)$ and $\overline{d}_+(1) = 1 + 20f/(27\beta_0)$ is the regular part of AD $d_+(n)$ in the limit $n \to 1$. Here n is the variable in Mellin space.

2.2 Effective slopes

As it has been shown in [14], the behaviour of PDFs and F_2 given in the Bessel-like form by generalized DAS approach can mimic a power law shape over a limited region of x and Q^2

$$f_a(x,Q^2) \sim x^{-\lambda_a^{\rm eff}(x,Q^2)} \;\;\text{and}\;\; F_2(x,Q^2) \sim x^{-\lambda_{\rm F_2}^{\rm eff}(x,Q^2)}.$$

The effective slopes $\lambda_a^{\rm eff}(x,Q^2)$ and $\lambda_{\rm F_2}^{\rm eff}(x,Q^2)$ have the form:

$$\begin{aligned} \lambda_{\rm F_2}^{\rm eff}(x,Q^2) &= \lambda_g^{\rm eff}(x,Q^2) \;=\; \frac{f_g^+(x,Q^2)}{f_g(x,Q^2)}\,\rho\,\frac{\tilde{I}_1(\sigma)}{\tilde{I}_0(\sigma)} \approx \rho - \frac{1}{4\ln(1/x)}, \\ \lambda_q^{\rm eff}(x,Q^2) &= \frac{f_q^+(x,Q^2)}{f_q(x,Q^2)}\,\rho\,\frac{\tilde{I}_2(\sigma)}{\tilde{I}_1(\sigma)} \approx \rho - \frac{3}{4\ln(1/x)}, \end{aligned} \tag{6}$$

where the symbol $\approx$ marks the approximation obtained in the expansion of the modified Bessel functions, when the "$-$" component is negligible. These approximations are accurate only at very large σ values (i.e. at very large Q^2 and/or very small x).

[3]The NLO results may be found in [14, 15].

2.3 Structure functions F_2^{cc} and F_2^{bb}

In the framework of the photon-gluon fusion (PGF) process, the SFs F_2^{cc} and F_2^{bb} have the following form [24]

$$F_2^{ii}(x,Q^2) \approx M_{2,g}^i(1,Q^2,\mu^2) f_g(x,\mu^2), \quad (i=c,b) \tag{7}$$

where $M_{2,g}^i(1,Q^2,\mu^2)$ is the first Mellin moment of the so-called gluon coefficient function $C_{2,g}^i(x,Q^2,\mu^2)$. AT LO, it has the form [24]

$$M_{2,g}^i(1,c) \;=\; \frac{2}{3}[1+2(1-c_i)J(c_i)] \tag{8}$$

with

$$J(c_i) = -\sqrt{b_i}\ln t_i, \qquad t_i = \frac{1-\sqrt{b_i}}{1+\sqrt{b_i}}, \qquad b_i = \frac{1}{1+4c_i}, \qquad c_i = \frac{m_i^2}{Q^2}. \tag{9}$$

3 Comparison with experimental data

Using the results of previous section we have analyzed HERA data for F_2 [1, 2] and F_2^{cc} [5, 7] and also the slope $\partial \ln F_2/\partial \ln(1/x)$ [3, 4] at small x from the H1 and ZEUS Collaborations. In order to keep the analysis as simple as possible, we fix $f=4$ and $\alpha_s(M_Z^2)=0.1166$ (i.e., $\Lambda^{(4)}=284$ MeV) in agreement with the recent ZEUS results in [1].

3.1 Structure function F_2

As it is possible to see in Figs. 1, 2 and 3, the twist-two approximation is reasonable at $Q^2 \geq 2\div 4$ GeV^2. At smaller Q^2, some modification of the approximation should be considered.

In Refs. [20, 21], to improve the agreement at small Q^2 values, we modifed the QCD coupling constant. We have found a good agreement with experimental data at essentially lower Q^2 values: $Q^2 \geq 0.5$ GeV^2 (see Figs. 1 and 2).

We considered two modifications.

In one case, which is more phenomenological, we introduce freezing of the coupling constant by changing its argument $Q^2 \to Q^2+M_\rho^2$, where M_ρ is the ρ-meson mass (see [20] and references therein). Thus, in the formulae of the Section 2 we should do the following replacement:

$$a_s(Q^2) \to a_{\rm fr}(Q^2) \equiv a_s(Q^2+M_\rho^2) \tag{10}$$

The second possibility incorporates the Shirkov–Solovtsov idea [25] about analyticity of the coupling constant that leads to the additional its power dependence. Then, in the formulae of the previous section the coupling constant $a_s(Q^2)$ should be replaced as follows: ($k=1$ and 2 at LO and NLO)

$$a_{\rm an}(Q^2) \;=\; a_s(Q^2) - \frac{1}{k\beta_0}\frac{\Lambda^2}{Q^2-\Lambda^2} + \dots\,, \tag{11}$$

where the symbol ... stands for terms which are zero and negligible at $Q \geq 1$ GeV [25] at LO and NLO, respectively.

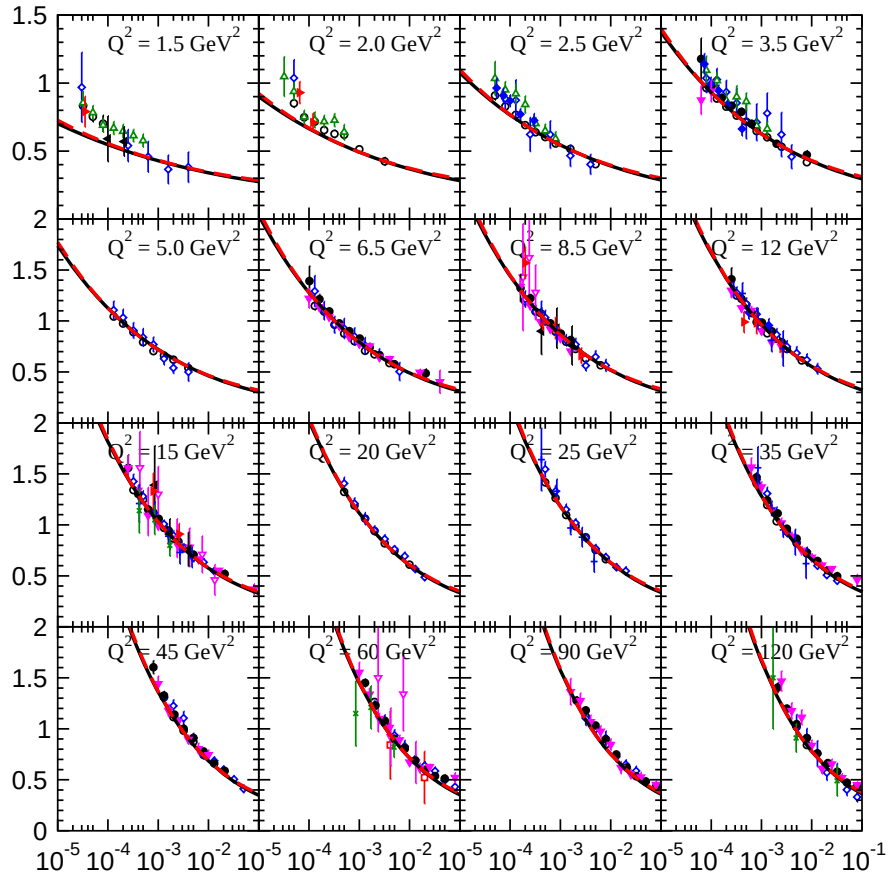

Figure 1: x dependence of $F_2(x, Q^2)$ in bins of Q^2. The experimental data from H1 (open points) and ZEUS (solid points) [1] are compared with the NLO fits for $Q^2 \geq 0.5$ GeV^2 implemented with the canonical (solid lines), frozen (dot-dashed lines), and analytic (dashed lines) versions of the strong-coupling constant.

3.2 Effective slopes

Figure 3 shows the experimental data for $\lambda_{F_2}^{\rm eff}(x, Q^2)$ at $x \sim 10^{-3}$, which represents an average of the x-values of HERA experimental data. The top dashed line represents the aforementioned linear rise of $\lambda(Q^2)$ with $\ln(Q^2)$. The Figs. 1, 2 and 3 demonstrate that the theoretical description of the small-Q^2 ZEUS data for $\lambda_{F_2}^{\rm eff}(x, Q^2)$ by NLO QCD is significantly improved by implementing the "frozen" and analytic coupling constants $\alpha_{\rm fr}(Q^2)$ and $\alpha_{\rm an}(Q^2)$, respectively, which in turn lead to very close results (see also [26]).

Indeed, the fits for $F_2(x, Q^2)$ in [15] yielded $Q_0^2 \approx 0.5$–0.8 GeV^2. So, initially we had $\lambda_{F_2}^{\rm eff}(x, Q_0^2) = 0$, as suggested by Eq. (1). The replacements of Eqs. (10) and (11) modify the value of $\lambda_{F_2}^{\rm eff}(x, Q_0^2)$. For the "frozen" and analytic coupling constants $\alpha_{\rm fr}(Q^2)$ and $\alpha_{\rm an}(Q^2)$, the value of $\lambda_{F_2}^{\rm eff}(x, Q_0^2)$ is nonzero and the slopes are quite close to the experimental data at $Q^2 \approx 0.5$ GeV^2. Nevertheless, for $Q^2 \leq 0.5$ GeV^2, Fig. 3 shows that there is still some disagreement with the data, which needs additional investigation.

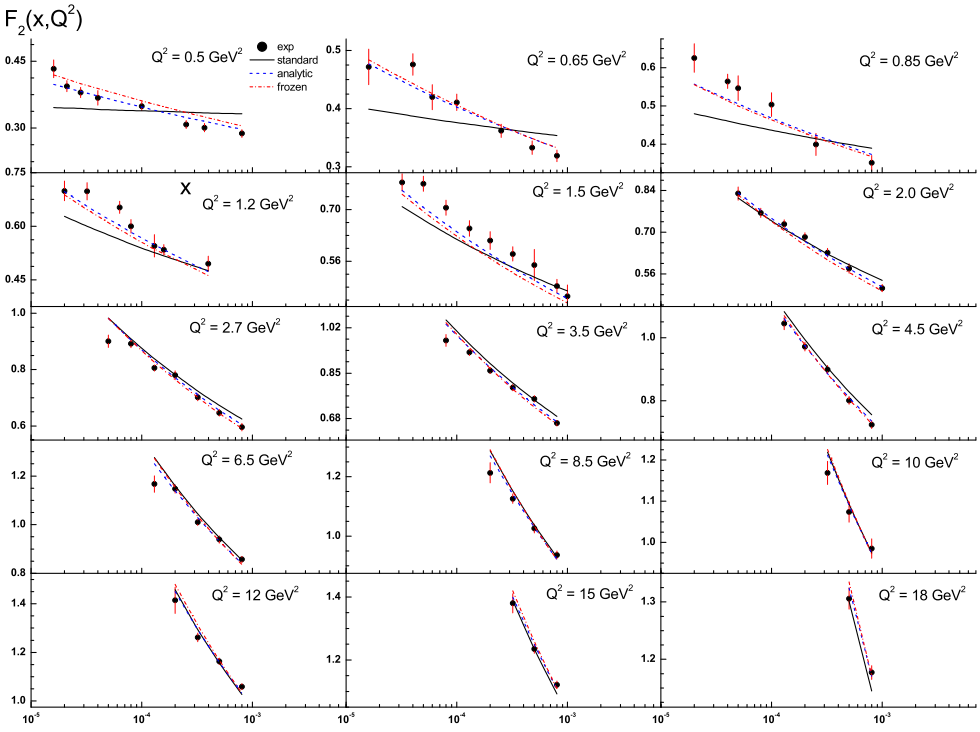

Figure 2: As in Fig.1 but for the combined H1&ZEUS exerimental data [2].

For comparison, we display in Fig. 3 also the results obtained by Kaidalov et al. [27] and by Donnachie and Landshoff [28] adopting phenomenological models based on Regge theory. While they yield an improved description of the experimental data for $Q^2 \leq 0.4$ GeV^2, the agreement generally worsens in the range 2 GeV$^2 \leq Q^2 \leq 8$ GeV^2.

The results of fits in [15, 20, 21] have an important property: they are very similar in LO and NLO approximations of perturbation theory. The similarity is related to the fact that the small-x asymptotics of the NLO corrections are usually large and negative (see, for example, α_s-corrections [29] to BFKL approach [30] [4]). Then, the LO form $\sim \alpha_s(Q^2)$ for some observable and the NLO one $\sim \alpha_s(Q^2)(1-K\alpha_s(Q^2))$ with a large value of K, are similar because $\Lambda \gg \Lambda_{\rm LO}$ [5] and, thus, $\alpha_s(Q^2)$ at LO is considerably smaller then $\alpha_s(Q^2)$ at NLO for HERA Q^2 values.

In other words, performing some resummation procedure (such as Grunberg's effective-charge method [31]), one can see that the NLO form may be represented as $\sim \alpha_s(Q^2_{\rm eff})$, where $Q^2_{\rm eff} \gg Q^2$. Indeed, from different studies [32, 26], it is well known that at small-x values the effective argument of the coupling constant is higher then Q^2.

[4] It seems that it is a property of any processes in which gluons, but not quarks play a basic role.

[5] The equality of $\alpha_s(M_Z^2)$ at LO and NLO approximations, where M_Z is the Z-boson mass, relates Λ and $\Lambda_{\rm LO}$: $\Lambda^{(4)} = 284$ MeV (as in ZEUS paper on [1]) corresponds to $\Lambda_{\rm LO} = 112$ MeV (see [15]).

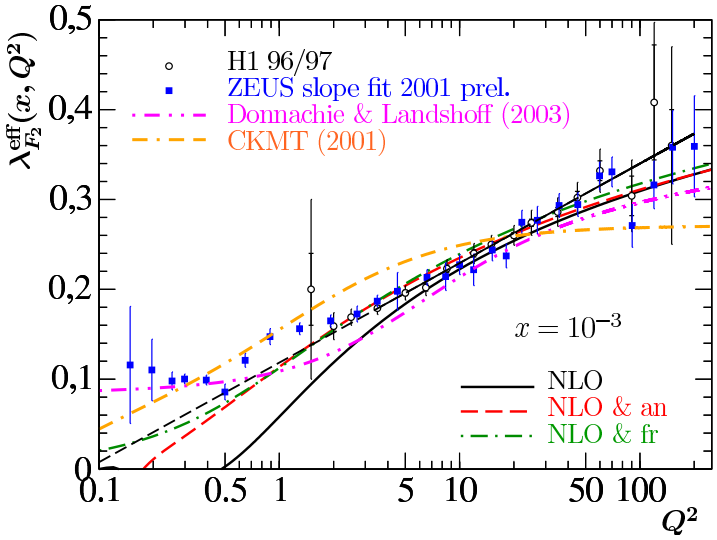

Figure 3: As in Fig,1 but for the Q^2 dependence of $\lambda_{F_2}^{\rm eff}(x,Q^2)$ for an average small-x value of $x = 10^{-3}$. The linear rise of $\lambda_{F_2}^{\rm eff}(x,Q^2)$ with $\ln Q^2$ [3] is indicated by the straight dashed line. For comparison, also the results obtained in the phenomenological models by Kaidalov et al. [27] (dash-dash-dotted line) and by Donnachie and Landshoff [28] (dot-dot-dashed line) are shown.

3.3 Structure function F_2^{cc}

We are now in a position to explore the phenomenological implications of our results for SF F_2^{cc}. As for our input parameters, we choose $m_c = 1.25$ GeV in agreement with Particle Data Group [34]. In order to fix the unphysical mass scale μ, we put $\mu^2 = Q^2 + 4m_c^2$, which is the standart scale in heavy quark production.

The PDF parameters μ_0^2, A_q and A_g shown in (1), have been fixed in the fits of F_2 experimental data (see the subsection 3.1). Their values depend on conditions chosen in the fits: the order of perturbation theory and the number f of active quarks.

Below b-quark threshold, the scheme with $f = 4$ has been used [15, 20] in the fits of F_2 data. Note, that the F_2 structure function contains F_2^{cc} as a part. In the fits, the NLO gluon density and the LO and NLO quark ones contribute to F_2^c, as the part of to F_2. Then, now in PGF scattering the LO coefficient function (9) corresponds in $m \to 0$ limit to the standart NLO Wilson coefficient (together with the product of the LO anomalous dimension γ_{qg} and $\ln(m_c^2/Q^2)$. It is a general situation, i.e. the coefficient funstion of PGF scattering at some order of perturbation theory corresponds to the standart DIS Wilson coefficient with the one step higher order. The reason is following: the standart DIS analysis starts with handbag diagram of photon-quark scattering and photon-gluon interaction begins at one-loop level.

Thus, in our F_2^{cc} analysis in the LO approximation of PGF process we should take $f_a(x,Q^2)$ extracted from fits of F_2 data at $f = 4$ and NLO approximation. In practice, in [22] we have applied our $f = 4$ NLO twist-two fit [15] of H1 data for F_2 with Q^2 cut: $Q^2 > 1.5$ GeV^2, which produces $Q_0^2 = 0.523$ GeV^2, $A_g = 0.060$ and $A_q = 0.844$.

The results for F_2^{cc} are prsented in Fig.4. We can see a good agreement between our compact formulas (7) and (9) and the modern experimental data [5, 6, 7] for F_2^{cc}. To keep place on Fig.4,

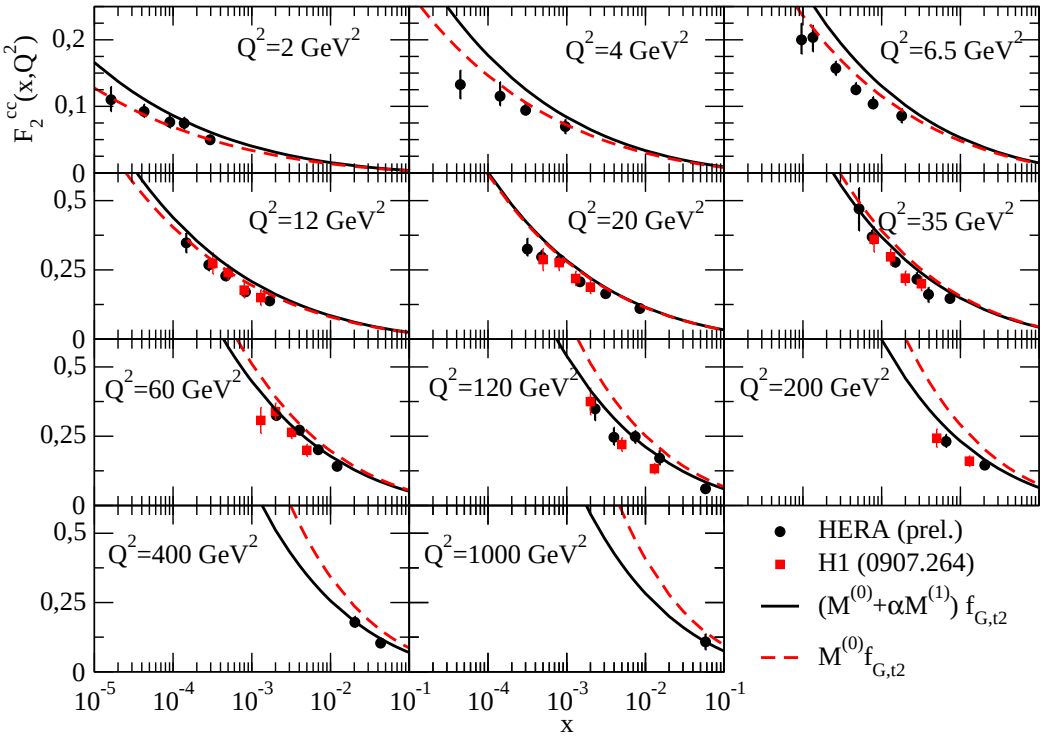

Figure 4: $F_2^{cc}(x,Q^2)$ evaluated as functions of x with the LO matrix elements (dashed lines) and with the NLO ones and with the factorization/renormalization scale $\mu^2 = Q^2 + 4m_c^2$ (solid lines). The black points and red squares correspond to the the combine H1ZEUS preliminary data [7] and H1 data [5], respectively.

we show only the H1 [5] data and the combine H1&ZEUS [7] one.

The good agreement between generalized double-asymptotic scaling DAS approach used here and F_2 and F_2^{cc} data demonstrates an equal importance of the both parton densities (gluon one and sea quark one) at low x. It is due to the fact that F_2 relates mostly to the sea quark distribution, while the F_2^{cc} relates mostly to the gluon one. Dropping sea quarks in analyse leads to the different gluon densities extracted from F_2 of from F_2^{cc} (see, for example, [33]).

4 Conclusions

We have shown the Q^2-dependence of the structure functions F_2 and F_2^{cc} and of the slope $\lambda_{F_2}^{\rm eff} = \partial \ln F_2 / \partial \ln(1/x)$ at small-x values in the framework of perturbative QCD. Our twist-two results are in very good agreement with precise HERA data at $Q^2 \geq 2$ GeV^2, where perturbative theory can be applicable. The application of the "frozen" and analytic coupling constants $\alpha_{\rm fr}(Q^2)$ and $\alpha_{\rm an}(Q^2)$ improves the agreement at small Q^2 values, $Q^2 \geq 0.5$ GeV^2.

For the slope $\lambda_{F_2}^{\rm eff}$ and for the structure function F_2^{cc}, our results agree with the corresponding experimental data [3, 4] and [5, 6, 7] well within errors without a free additional parameters. In the Q^2 range probed by the HERA data, our NLO predictions agree very well with the

LO ones. Since we worked in the fixed-flavour-number scheme, our results for F_2^{cc} are bound to break down for $Q^2 \gg 4m_c^2$, which manifests itself by appreciable QCD correction factors and scale dependences. As is well known, this problem is conveniently solved by adopting the variable-flavour-number scheme, which not considered here.

As a next step of investigations, we plan to add the BFKL corrections to our approach [14] (see appendix A in [35]) and to use our approach to analyse the cross sections of processes studied at LHC by analogy with our investigations [36] of the total cross section of ultrahigh-energy deep-inelastic neutrino-nucleon scattering.

A.V.K. thanks the Organizing Committee of the Helmholtz International Summer School "Physics of Heavy Quarks and Hadrons - 2013" for invitation and support. This work was supported in part by RFBR grant 13-02-01005-a.

References

[1] C. Adloff *et al.*, H1 Coll., Nucl.Phys. B497 (1997) 3; Eur.Phys.J. C21 (2001) 33; S. Chekanov *et al.*, ZEUS Coll., Eur.Phys.J. C21 (2001) 443.

[2] F.D. Aaron *et al.*, H1 and ZEUS Coll., JHEP 1001 (2010) 109.

[3] C. Adloff *et al.*, H1 Coll., Phys.Lett. B520 (2001) 183.

[4] T. Lastovicka, H1 Coll., Acta Phys.Polon. B33 (2002) 2835; B. Surrow, ZEUS Coll., hep-ph/0201025.

[5] F. D. Aaron *et al.*, H1 Coll., Phys. Lett. B686 (2010) 91; Eur. Phys. J. C65 (2010) 89.

[6] H. Abramowicz *et al.*, ZEUS coll., Eur. Phys. J. C69 (2010) 347; S. Chekanov *et al.*, ZEUS Coll., Eur. Phys. J. C65 (2010) 65.

[7] H. Abramowicz *et al.*, H1 and ZEUS Coll., Eur. Phys. J. C73 (2013) 2311.

[8] V.N. Gribov and L.N. Lipatov, Sov.J.Nucl.Phys. 15 (1972) 438, 675; L.N. Lipatov, Sov. J. Nucl. Phys. 20 (1975) 94; G. Altarelli and G. Parisi, Nucl.Phys. B126 (1977) 298; Yu.L. Dokshitzer, Sov. Phys. JETP 46 (1977) 641.

[9] A.M. Cooper-Sarkar *et al.*, Int.J.Mod.Phys. A13 (1998) 3385; A.V. Kotikov, Phys.Part.Nucl. 38 (2007) 1; [Erratum-ibid. 38 (2007) 828].

[10] W.K. Tung *et al.*, STEQ Coll., JHEP 0702 (2007) 053; A.D. Martin *et al.*, Phys.Lett. B652 (2007) 292; M. Gluck *et al.*, Phys.Rev. D77 (2008) 074002; S. Alekhin *et al.*, Phys.Rev. D81 (2010) 014032.

[11] A.V. Kotikov *et al.*, Z.Phys. C58 (1993) 465; G. Parente *et al.*, Phys.Lett. B333 (1994) 190; A.L. Kataev *et al.*, Phys.Lett. B388 (1996) 179; Phys.Lett. B417 (1998) 374; Nucl.Phys. B573 (2000) 405; A.V. Kotikov and V.G. Krivokhijine, Phys.At.Nucl. 68 (2005) 1873; B.G. Shaikhatdenov *et al.*, Phys.Rev. D81 (2010) 034008.

[12] R.D. Ball and S. Forte, Phys.Lett. B336 (1994) 77.

[13] L. Mankiewicz *et al.*, Phys.Lett. B393 (1997) 175.

[14] A. V. Kotikov and G. Parente, Nucl.Phys. B549 (1999) 242.

[15] A. Yu. Illarionov *et al.*, Phys.Part.Nucl. 39 (2008) 307.

[16] A. De Rújula *et al.*, Phys.Rev. D10 (1974) 1649.

[17] M. Arneodo *et al.*), NM Coll., Phys.Lett. B364 (1995) 107; Nucl.Phys. B483 (1997) 3; M.R. Adams *et al.*, E665 Coll., Phys.Rev. D54 (1996) 3006; A. Donnachie and P. V. Landshoff, Nucl.Phys. B244 (1984) 322; B267 (1986) 690; Z.Phys. C61 (1994) 139.

[18] J. Breitweg *et al.*, ZEUS Coll., Phys.Lett. B407 (1997) 432.

[19] J. Breitweg *et al.*, ZEUS Coll., Phys.Lett. B487 (2000) 53; Eur.Phys.J. C21 (2001) 443.

[20] G. Cvetic *et al.*, Phys.Lett. B679 (2009) 350.

[21] A. V. Kotikov and B. G. Shaikhatdenov, Phys. Part. Nucl. 44 (2013) 543.

[22] A. Y. .Illarionov and A. V. Kotikov, Phys. Atom. Nucl. 75 (2012) 1234.

[23] A.V. Kotikov and G. Parente, J. Exp. Theor. Phys. 97 (2003) 859.

[24] A. Y. Illarionov, B. A. Kniehl and A. V. Kotikov, Phys. Lett. B663 (2008) 66.

[25] D.V. Shirkov and I.L. Solovtsov, Phys.Rev.Lett 79 (1997) 1209.

[26] A.V. Kotikov *et al.*, J. Exp. Theor. Phys. 101 (2005) 811; Phys. Atom. Nucl. 75XS (2012) 507.

[27] A.B. Kaidalov *et al.*, Eur.Phys.J. C20 (2001) 301;

[28] A. Donnachie and P.V. Landshoff, Acta Phys.Polon. B34 (2003) 2989.

[29] V. S. Fadin and L. N. Lipatov, Phys.Lett. B429 (1998) 127; G. Camici and M. Ciafaloni, Phys.Lett. B430 (1998) 349; A.V. Kotikov and L.N. Lipatov, Nucl.Phys. B582 (2000) 19.

[30] L.N. Lipatov, Sov.J.Nucl.Phys. 23 (1976) 338; V.S. Fadin *et al.*, Phys.Lett. B60 (1975) 50; E.A. Kuraev *et al.*, Sov. Phys. JETP 44 (1976) 443; 45 (1977) 199; I.I. Balitsky and L.N. Lipatov, Sov.J.Nucl.Phys. 28 (1978) 822; JETP Lett. 30 (1979) 355.

[31] G. Grunberg, Phys.Rev. D29 (1984) 2315; Phys.Lett. B95 (1980) 70.

[32] Yu.L. Dokshitzer and D.V. Shirkov, Z.Phys. C67 (1995) 449; A.V. Kotikov, Phys.Lett. B338 (1994) 349; W.K. Wong, Phys.Rev. D54 (1996) 1094; S.J. Brodsky *et al.*, JETP. Lett. 70 (1999) 155; M. Ciafaloni *et al.*, Phys.Rev. D60 (1999) 114036; G. Altarelli *et al.*, Nucl.Phys. B621 (2002) 359; Bo Andersson *et al.*, Eur.Phys.J. C25 (2002) 77.

[33] H. Jung *et al.*, arXiv:0706.3793 [hep-ph]; arXiv:hep-ph/0611093.

[34] C. Amsler *et al.*, Particle Data Group, Phys. Lett. B667 (2008) 1.

[35] A. V. Kotikov, PoS Baldin -ISHEPP-XXI (2012) 033 [arXiv:1212.3733 [hep-ph]].

[36] R. Fiore *et al.*, Phys.Rev. D73 (2006) 053012; Phys.Rev. D71 (2005) 033002; Phys.Rev. D68 (2003) 093010; A. Y. Illarionov *et al.*, Phys.Rev.Lett. 106 (2011) 231802.